$pd \leftrightarrow \pi^+ t$ reaction around the Δ resonance

L. Canton

Istituto Nazionale di Fisica Nucleare, Sezione di Padova, Via F. Marzolo 8, I-35131 Padova, Italy

W. Schadow

Physikalisches Institut der Universität Bonn, Endenicher Allee 11-13, D-53115 Bonn, Germany

The $pd \leftrightarrow \pi^+ t$ process has been calculated in the energy region around the Δ resonance with elementary production/absorption mechanisms involving one and two nucleons. The isobar degrees of freedom have been explicitly included in the two-nucleon mechanism via π- and ρ-exchange diagrams. No free parameters have been employed in the analysis since all the parameters have been fixed in previous studies on the simpler $pp \leftrightarrow \pi^+ d$ process. The treatment of the few-nucleon dynamics entailed a Faddeev-based calculation of the reaction, with continuum calculations for the initial p-d state and accurate solutions of the three-nucleon bound-state equation. The integral cross section was found to be quite sensitive to the NN interaction employed while the angular dependence showed less sensitivity. Approximately a 4% effect was found for the one-body mechanism, for the three-nucleon dynamics in the p-d channel, and for the inclusion of a large, possibly converged, number of three-body partial states, indicating that these different aspects are of comparable importance in the calculation of the spin-averaged observables. [S0556-2813(97)01409-X]

PACS number(s): 25.80.Ls, 25.10.+s, 13.75.Cs

I. INTRODUCTION

Pion production/absorption on nuclear systems represents a complex, challenging problem; a fact known for many years. In an attempt to explain the multitude of experimental results collected over more than 40 years, many different theoretical approaches have been proposed, with the aim of improving our understanding of these reactions and, more generally, of the hadronic phenomena.

The simplest approaches which have been employed assume a one-nucleon mechanism originated by the πNN vertex (generally — but not always — a Galilei invariant non-relativistic reduction of the usual γ_5 pion-nucleon interaction) and recast the transition amplitude in a distorted-wave impulse approximation (DWIA) formalism where the many-body aspects can be treated with different levels of approximations [1]. First-order corrections from the π-nucleus multiple scattering series leads to the two-nucleon mechanisms where a pion emitted from one nucleon scatters from another before leaving the whole nucleus.

The nonperturbative character of the hadronic interactions, together with the energy-momentum mismatch which forbids absorption on single, free nucleons and suppresses one-nucleon absorption on bound nucleons, makes these re-scattering effects an important aspect which cannot be ignored for the reproduction of low-energy data. At the Δ resonance, however, most of the assumptions used in the early calculations were not applicable, and other phenomenological approaches have been developed.

A relevant success was encountered by the ``deuteron'' model, originally employed by Ruderman [2], where the $pd \rightarrow \pi^+ t$ cross section is directly linked to the $pp \rightarrow \pi^+ d$ experimental cross section, by means of suitable nuclear structure functions. This method has the considerable advantage of disentangling the question of the choice of the correct interaction mechanisms from the knowledge of the bound-state wave functions. The theoretical uncertainties about the interaction mechanisms at the resonance are simply bypassed through the employment of the experimental $pp \rightarrow \pi^+ d$ cross section. The approach has been later refined by several authors, who addressed the main issues such as the role of the distortion effects, sensitivity of the results with respect to the available model wave functions, and generalization of the formalism from three-baryon systems to the many-nucleon $A(p, \pi^+)A+1$ case. A partial but representative sample of works developed along these lines is given in Refs. [3–5].

More recently, the analysis of the $A(p, \pi^+)A+1$ reaction in terms of the $pp \rightarrow \pi^+ d$ process has been extended to spin observables by Falk [6], by using the $pp \rightarrow \pi^+ d$ amplitude analysis of Bugg *et al.* [7], rather than the averaged cross-section data of earlier works. In most cases, an overall fair, qualitative agreement with the trend of the large bulk of experimental data has been found, indicating that the deuteron model even in its spin-dependent version may be considered a starting point for phenomenological studies which include spin-polarization data. This kind of approach, however, suffers from a number of problems which limits possible future refinements and demands for more appropriate theoretical formulations. First, the model considers NN production mechanisms limited to the (dominant) $1 \rightarrow 0$ isospin transition, while a complete model should take into account also the effects in the remaining isospin channels. Second, the amplitudes used for input are on-shell quantities, while in theory the off-shell effects should be taken into account. Third, there is a certain arbitrariness in the kinematical constraints which define the energy parameter for the evaluation of the input $2N$ production amplitude; because of that, the results are not uniquely determined. And finally, in practically all applications the distortion contributions are in danger of double countings; indeed, in the evaluation of the

distortion effects one should subtract the distortion contributions on the active pair, which are already included in the $pp \rightarrow \pi^+ d$ data.

To overcome these limitations, and to challenge the validity of the ''deuteron'' approaches, there has been a number of papers where more microscopic models have been suggested [8–10]. Here, the dynamical input was not mediated or hidden by the cross-section data, but consists of nonrelativistic interactions among pions, nucleons, and isobars. In particular, the coupled ΔN dynamics is obtained through the solution in R space of the two-baryon Schrödinger equation. First calculations [8] employed simple s-wave deuteron and triton wave functions of uncorrelated Gaussian forms, and were extremely limited in the number of intermediate states included in the calculation. Subsequent analyses [9,10] used better parametrizations (including d states) for the nuclear wave functions, and increased slightly (from 1 to 4 or 5) the number of two-body angular-decomposed intermediate states, finding that these aspects improve the calculated angular distributions without, however, finding an agreement with theory and experiments, especially for the results at large angles, where considerable discrepancies persist. One of the conclusions from these studies was that these microscopic calculations needed important improvements in order to give a good reproduction in the normalization and in the angular distributions, and that these improvements would lead to enormous complications in the theoretical evaluation of the observables.

In an attempt to go beyond the description of meson production in terms of single-nucleon and two-nucleon mechanisms [11], it was shown that meson double rescattering could be a good candidate to account for the discrepancies at backward angles, particularly in the energy region above the Δ resonance. However, the bulk results, while moving towards the right direction, were still far from being optimal and this again poses the question of the need to overcome the various technical approximations which had to be assumed to keep the calculation tractable. The study has the merit to address the attention to the problem of three-body mechanisms in meson production/absorption, and this is still an open question which we hope will be theoretically disentangled in the near future with the help of the results collected in recent years by pion-absorption experiments with large angular detector systems [12–14] and by making comparative analyses in the Δ region with the phenomenology of ^{3}He photodisintegration [15].

In this paper, we have calculated the excitation function and differential cross section for the $pd \rightarrow \pi t$ reaction in the Δ region by using single-nucleon and two-nucleon mechanisms. In particular, the two-nucleon mechanism explicitly refers to the intermediate isobar excitation with $\pi + \rho$ exchange ΔN-NN transitions with tensor components. The one-body mechanism is mediated by the πNN vertex, while the two-body process is triggered by the $\pi \Delta N$ one. The two mechanisms have been decomposed in complete three-nucleon partial waves, while the asymptotic pion-nucleus plane wave has been kept three dimensional. This choice leads to matrix elements with a large number of couplings between different three-body states and the technical complications involved have been kept under control with a great deal of numerical analysis. Also the intermediate three-

baryon (ΔNN) state has been represented in partial waves with inclusion of angular momenta up to $l=2$ for the ΔN subsystem. However, in preliminary test calculations [16], the quality of the convergence has been checked up to $l=5$. The antisymmetrization prescription for the three nucleons has been fully taken into account via the formalism of the permutation operators [17] and brings into the theory further mechanisms which differ from the leading ones by exchange diagrams. The matrix elements of the symmetrization permutator P involve a large number of couplings between different three-nucleon partial waves, and rather than invoking a drastic reduction of the number of states, we have accepted the fact that we have to deal with the numerical difficulties implied by the approach.

Following the formalism developed in Ref. [17] we have embedded these absorption operators in a Faddeev-based treatment of the three-nucleon dynamics. Accurate bound-state wave functions have been obtained with high-rank Faddeev-AGS calculations, and a suitable generalization of the quasiparticle method to absorption processes has been formulated in order to take into account the three-nucleon dynamics in the pd channel. This continuum calculation has been performed in the rank-one (separable) approximation and therefore is not as accurate as the bound-state wave function, but this is the first calculation which, to our knowledge, includes a Faddeev-based treatment of the initial-state three-body dynamics for the $pd \rightarrow \pi + t$ process (and the other processes related by isospin symmetry).

Because of the above-mentioned reasons, we think that the treatment illustrated in this work achieves several improvements with respect to the previous, pioneering, microscopic analyses. We have devoted Sec. II to further discussions on these and other important aspects of our calculations, such as the treatment of the Δ mass and width in the intermediate three-body (ΔNN) Green's function, and the inclusion of off-shell effects (for this second aspect, see also the discussion at the beginning of Sec. III). The remaining part of Sec. III compares the results of our analysis with experiments and Sec. IV contains a brief summary and the conclusions.

II. THEORY

We express the transition amplitude for the $\pi^+ t \leftrightarrow pd$ reaction by the following matrix element:

$$A_d^{\text{tot}} = {}_\mathcal{S}\langle \Psi_d^{(-)} | \mathcal{A} | \Psi_{\text{BS}} \rangle_\mathcal{S} | \mathbf{P}_0^\pi \rangle, \tag{1}$$

where $|\Psi_{\text{BS}}\rangle_\mathcal{S}$ represents the three-nucleon bound state (BS) and ${}_\mathcal{S}\langle \Psi_d^{(-)}|$ the three-body continuum state with ingoing boundary condition and with the deuteron d in the asymptotic channel. Both states are assumed to be properly antisymmetrized in the nucleonic coordinates and the state $|\mathbf{P}_0^\pi\rangle$ is the pion-nucleus three-dimensional plane wave. In a previous exploratory calculation [16] the bound-state wave function calculated in Ref. [18] was used. That wave function originally was determined in Ref. [18] by solving the Faddeev equation with the Paris potential and with explicit allowance of the Δ degrees of freedom and consisted of 48 three-baryon partial waves, of which 22 refer to purely nucleonic states. Because of the smallness of the remaining

isobar states, only the nucleonic states were retained in the calculation of Ref. [16]. In the present calculation, we have independently recalculated the three-nucleon bound state for various realistic nuclear potentials, and the details of these calculations are illustrated in Sec. II B.

The absorption mechanisms are specified by the operator $\mathcal{A}$. To avoid double countings, we avoided purely nucleonic intermediate states in $\mathcal{A}$. This is because we calculate the final-state interactions among the three nucleons using realistic NN potentials, without performing any kind of subtraction in the nuclear potential.

In this study we consider absorption mechanisms generated by pion-nucleon interactions in p waves as described by the $\pi N \Delta$ and πNN vertices. The nonrelativistic interaction Hamiltonians are

$$H_{\pi N \Delta} = \frac{f_{\pi N \Delta}}{m_\pi} \int d\mathbf{r} \rho(\mathbf{r}) (\vec{S} \cdot \vec{\nabla})(\vec{\Phi}(\mathbf{r}) \cdot \vec{T}), \qquad (2)$$

for the $\pi N \Delta$ interaction, and

$$H_{\pi NN} = \frac{f_{\pi NN}}{m_\pi} \int d\mathbf{r} \rho(\mathbf{r})(\vec{\sigma} \cdot \vec{\nabla})(\vec{\Phi}(\mathbf{r}) \cdot \vec{\tau}), \qquad (3)$$

for the πNN one. Here, the baryonic density is denoted by $\rho(\mathbf{r})$, while $\vec{\Phi}(\mathbf{r})$ is the pionic isovector field. The quantities M and m_π are the nucleon and pion masses, respectively, while $\vec{\sigma}$ and $\vec{\tau}$ are the nucleon spin and isospin operators, and $\vec{S}$ and $\vec{T}$ are the corresponding generalization to the isobar-nucleon transition.

The πNN vertex defines the simplest one-body absorption mechanism and is sometimes referred to as the impulse approximation (IA) mechanism. However, this is suppressed because of energy-momentum mismatch, therefore two-nucleon mechanisms dominate. These are taken into account through the Δ-rescattering process, where the πNN-NN inelasticities are modeled through a $\pi N \Delta$-ΔN–NN two-step transition. Here the first transition is triggered by the $\pi N \Delta$ vertex given above, followed by an intermediate ΔN propagation and by the ΔN-NN transition. The intermediate propagation of the isobar is described by the Green's function

$$G_0 = \frac{1}{E + M - \mathcal{M}_\Delta - p^2/2\mu_\Delta - q^2/2\nu_\Delta}, \qquad (4)$$

where E is given by the pion energy plus the target kinetic energy in the c.m. system. The Jacobi variables p and q are the pair ΔN and spectator nucleon momenta, respectively. Correspondingly, μ_Δ and ν_Δ are the reduced masses of the pair and spectator-pair systems. $\mathcal{M}_\Delta - M$ is the isobar-nucleon mass gap. Since the Δ isobar is not a stable particle but a resonance, its mass is endowed with an imaginary part Γ_Δ, associated to the decay width of the isobar

$$\mathcal{M}_\Delta = M_\Delta - E_s - \frac{i}{2}\Gamma_\Delta(E), \qquad (5)$$

with $M_\Delta = 1232$ (MeV) and E_s being the energy-shift parameter. The energy dependence for Γ has been modeled

phenomenologically in a previous analysis of the $\pi d \leftrightarrow pp$ reaction [19]. Here we use the same analytical expression which was obtained in that analysis, with the Γ_Δ energy dependence extracted by the condition

$$\sigma(E) = \frac{D}{(E - E_R)^2 + \Gamma_\Delta(E)^2/4}, \qquad (6)$$

where $\sigma(E)$ is the experimental excitation function for pion absorption on deuterons. In the numerical calculation, the fit to $\sigma(E)$ obtained by Ritchie [20] is used.

In a meson-exchange framework [21,22], the $N\Delta$-NN transition potential can be obtained from the π- and ρ-exchange diagrams

$$V_{N\Delta} = (V_{N\Delta}^\pi + V_{N\Delta}^\rho)(\vec{T}_1^\dagger \cdot \vec{\tau}_2),$$

$$V_{N\Delta}^\pi = -\frac{g_\pi f_{\pi N\Delta}}{2Mm_\pi}(\vec{S}_1^\dagger \cdot \vec{Q})(\vec{\sigma}_2 \cdot \vec{Q})G(\omega_\pi),$$

$$V_{N\Delta}^\rho = -\frac{(g_\rho + f_\rho)f_{\rho N\Delta}}{2Mm_\rho}(\vec{S}_1^\dagger \times \vec{Q}) \cdot (\vec{\sigma}_2 \times \vec{Q})G(\omega_\rho). \quad (7)$$

The operator $\vec{Q}$ is the baryon-baryon transferred momentum, m_ρ is the mass of the ρ-meson, and the function $G(\omega)$, which describes the meson-exchange propagation, takes into account the mass difference between nucleons and isobars:

$$G(\omega) = \frac{1}{2\omega^2} + \frac{1}{2\omega(M_\Delta - M + \omega)}$$

$$\simeq \frac{1}{2\omega^2} + \frac{1}{2\omega^2 + 2m_\pi(M_\Delta - M)}. \qquad (8)$$

Here, ω is the relativistic energy of the exchanged meson and, as shown in the last expression, we have taken into account the ΔN mass difference in an approximated way in order to obtain analytical expressions when performing the partial-wave expansion. Each meson-baryon coupling in the transition potential has been endowed with a phenomenological form factor of monopole type, with the exclusion of the $\rho N\Delta$ coupling, where a dipole-type form factor was assumed.

Finally, we discuss how the three-nucleon dynamics can be incorporated into the theory, or equivalently, how we calculate $_s\langle \Psi_d^{(-)}|$. The method is similar to previous procedures developed to incorporate final-state interactions (FSI) in the photodisintegration of three-body systems [23–25,27,28]. First, we introduce the operator P_{23} which exchanges spin, isospin, and position coordinates of nucleons 2 and 3. We then introduce the cyclic and anticyclic permutation operators P_2 and P_3, respectively. They exchange the global coordinates of the three nucleons in the following manner: $123 \rightarrow 231$ and $123 \rightarrow 312$, and can be expressed in term of the pair exchange operators as $P_2 \equiv P_{12}P_{23}$ and $P_3 \equiv P_{13}P_{23}$. This leads to the full permutator

$$P \equiv P_2 + P_3, \qquad (9)$$

and to the normalized symmetrizer $S \equiv (1+P)/\sqrt{3}$. It is now possible to derive the complete wave function in terms of the asymptotic channel wave function $_1\langle\Phi_d|$ (the subscript 1 denotes antisymmetrization with respect to the pair made of nucleons labeled 2 and 3)

$$_S\langle\Psi_d^{(-)}| = {_1}\langle\Phi_d|(1+\mathbf{T}G_0)S, \qquad (10)$$

where the three-body operator $\mathbf{T}$ satisfies a Faddeev-like equation

$$\mathbf{T} = Pt + PtG_0\mathbf{T} \qquad (11)$$

(t is the two-nucleon t-matrix). We now define the Møller operator $\Omega^{(-)\dagger} \equiv 1 + \mathbf{T}G_0$, in which case

$$_S\langle\Psi_d^{(-)}| = {_1}\langle\Phi_d|\Omega^{(-)\dagger}S. \qquad (12)$$

This operator satisfies the Faddeev-like equation

$$\Omega^{(-)\dagger} = 1 + PtG_0\Omega^{(-)\dagger}, \qquad (13)$$

with which the pion-disintegration amplitude can be rewritten as

$$A_d = {_1}\langle\Phi_d|\Omega^{(-)\dagger}S\mathcal{A}|\Psi_{\mathrm{BS}},\mathbf{P}_0^\pi\rangle. \qquad (14)$$

Because of the two equations above, the full amplitude satisfies the integral equation

$$A_d = {_1}\langle\Phi_d|S\mathcal{A}|\Psi_{\mathrm{BS}},\mathbf{P}_0^\pi\rangle + {_1}\langle\Phi_d|PtG_0\Omega^{(-)\dagger}S\mathcal{A}|\Psi_{\mathrm{BS}},\mathbf{P}_0^\pi\rangle. \qquad (15)$$

The first term on the right-hand side corresponds to the plane-wave contributions, while in the second term the NN rescatterings (to all orders) are singled out.

As is well known, when the two-body transition matrix is represented in a separable form, the Alt-Grassberger-Sandhas (AGS) equations [26] for neutron-deuteron scattering reduce to effective two-body Lippmann-Schwinger equations. The same happens for the calculation of final-state interaction effects in the photodisintegration of the triton ($\gamma + t \rightarrow n + d$) [23–25,27,28], where one obtains a similar effective two-body Lippmann-Schwinger equation, the only difference being that the driving term of the n-d scattering equation (i.e., the particle-exchange diagram, the so-called ''Z diagram'') is replaced by the off-shell extension of the plane-wave photoabsorption amplitude. Here, we use a similar scheme for pion absorption on the three-nucleon systems.

In order to accomplish this, we use the separable expansion method proposed by Ernst, Shakin, and Thaler (EST) [32] for representing a given NN interaction. The EST method is very reliable and has been tested in the past for bound-state [33,34] and scattering calculations [35–37]. In this approximation the original interaction is expressed in separable terms of the form

$$V = \sum_{\mu,\nu=1}^{N} |f_\mu\rangle\Lambda_{\mu\nu}\langle f_\nu|, \qquad (16)$$

where N is the rank of the approximation. The detailed structure of the potential, the parameters for the form factors

$|f_\mu\rangle$, and the interaction strength λ can be found in Refs. [36,37]. The input two-body transition matrix t is given as a series of separable terms

$$t = \sum_{\mu\nu} |f_\mu\rangle\Delta_{\mu\nu}\langle f_\nu|. \qquad (17)$$

To simplify the notation, we restrict the sum above to just one value for the indices μ and ν, so that the transition matrix takes the rank-one form $t = |f_1\rangle\Delta\langle f_1|$. In Δ as well as in the form factor $|f_1\rangle$, we have also omitted the proper energy dependence, but it must be remembered that when the two-body t matrix is embedded in the three-particle space the correct energy dependence is upon $E-(3q^2/4M)$, where the energy of the spectator nucleon has to be subtracted. The separable representation reproduces the correct negative-energy bound-state pole of the two-body t matrix (for the deuteron quantum numbers) if the form factor satisfies the homogeneous equation

$$VG_0(E_d)|f_1\rangle = |f_1\rangle, \qquad (18)$$

and, within a normalization factor, $G_0(E_d)|f_1\rangle$ is the deuteron wave $|\Phi_d\rangle$.

Use of the separable representation of the t-matrix input in the integral equation (15) leads to the effective two-body equation

$$A(q,E) = B(q,E) + \int q'^2 dq' V(q,q',E)$$
$$\times \Delta\left(E - \frac{3q'^2}{4M}\right) A(q',E), \qquad (19)$$

with the definitions

$$A(q,E) = {_1}\langle f_1,q|G_0^{(+)}\Omega^{(-)\dagger}S\mathcal{A}|\Psi_{\mathrm{BS}},\mathbf{P}_0^\pi\rangle,$$

$$B(q,E) = {_1}\langle f_1,q|G_0^{(+)}S\mathcal{A}|\Psi_{\mathrm{BS}},\mathbf{P}_0^\pi\rangle,$$

$$V(q,q',E) = {_1}\langle f_1,q|G_0^{(+)}P|f_1,q'\rangle_1. \qquad (20)$$

Here, A and B represent the off-shell extension for the full and plane-wave pion-absorption amplitudes, respectively, while V is the effective two-body potential which represents the one-particle exchange diagram between different sub-cluster rearrangements.

These amplitudes are decomposed in three-nucleon partial waves, while the pion-nucleus incident wave is treated in three dimensions. Details on the employed representation were given elsewhere [17]. The representation of the three-body states is defined in momentum space and the partial-wave decomposition is discussed within the jI coupling scheme. The index α refers to the whole set of quantum numbers [i.e., orbital momentum, spin, total angular momentum, and isospin of the pair $(ls)j;t$, of the spectator $(\lambda\sigma)I;\tau$, total angular momentum, isospin, and associated third components $JJ^z;TT^z$].

The absorption mechanisms we include in our calculation have the following structure:

$$B_E^\Delta(q',\alpha',E) = 2\sqrt{3} \sum_{\alpha'',\alpha_\Delta,\alpha} \int p'^2 dp' \, p''^2 dp'' q''^2 dq'' p_\Delta^2 dp_\Delta p^2 dp q^2 dq$$

$$\times \frac{f_1(\alpha',p') \langle p'q'\alpha'|P|p''q''\alpha''\rangle}{E-(3/4)q'^2/M - p'^2/M + i\epsilon} \frac{\langle p''q''\alpha''|V_{N\Delta}|p_\Delta q''\alpha_\Delta\rangle}{E+(M-\mathcal{M}_\Delta) - q''^2/2\nu_\Delta - p_\Delta^2/2\mu_\Delta} \langle p_\Delta q''\alpha_\Delta|H_{\pi N\Delta}|pq\alpha\rangle\langle pq\alpha|\Psi_{\text{BS}}\rangle,$$

(21)

and

$$B_D^\Delta(q',\alpha',E) = 2\sqrt{3} \sum_{\alpha_\Delta,\alpha} \int p'^2 dp' \, p_\Delta^2 dp_\Delta p^2 dp q^2 dq \frac{f_1(\alpha',p')}{E-(3/4)q'^2/M - p'^2/M + i\epsilon} \frac{\langle p'q'\alpha'|V_{N\Delta}|p_\Delta q'\alpha_\Delta\rangle}{E+(M-\mathcal{M}_\Delta) - q'^2/2\nu_\Delta - p_\Delta^2/2\mu_\Delta}$$

$$\times \langle p_\Delta q'\alpha_\Delta|H_{\pi N\Delta}|pq\alpha\rangle\langle pq\alpha|\Psi_{\text{BS}}\rangle$$

(22)

for the Δ-rescattering mechanisms, and

$$B_E^{\text{IA}}(q',\alpha',E) = \sqrt{3} \sum_{\alpha'',\alpha} \int p'^2 dp' \, p''^2 dp'' q''^2 dq'' p^2 dp q^2 dq \frac{f_1(\alpha',p')\langle p'q'\alpha'|P|p''q''\alpha''\rangle}{E-(3/4)q'^2/M - p'^2/M + i\epsilon} \langle p''q''\alpha''|H_{\pi NN}|pq\alpha\rangle\langle pq\alpha|\Psi_{\text{BS}}\rangle,$$

(23)

$$B_D^{\text{IA}}(q',\alpha',E) = \sqrt{3} \sum_\alpha \int p'^2 dp' \, p^2 dp q^2 dq \frac{f_1(\alpha',p')\langle p'q'\alpha'|H_{\pi NN}|pq\alpha\rangle\langle pq\alpha|\Psi_{\text{BS}}\rangle}{E-(3/4)q'^2/M - p'^2/M + i\epsilon},$$

(24)

for the one-body IA mechanisms. Clearly, all these mechanisms add coherently to give the total amplitude. The subscripts E and D differentiate between exchange and direct mechanisms, respectively. The D mechanisms correspond to the probability that nucleon 1 is the free nucleon in the outgoing channel (hence nucleons 2 and 3 form a deuteron) while the other two cases (i.e., nucleon 2 or 3 as free outgoing particle) are assembled together in the E mechanisms. These exchanges in the rearrangement channel are performed by the permutation operator P. We refer to the appendix of Ref. [29] for details on the partial-wave matrix elements for this operator. Each Δ-rescattering mechanism is multiplied by the factor $2\sqrt{3}$ which arises from the multiplicity of the possible two-body mechanisms and by the normalization factor due to Pauli principle. The same considerations lead to the factor $\sqrt{3}$ in the impulse approximation. We also observe that a coupled-channel structure has to be intended for the deuteron form factor $f_1(\alpha',p)$, since the deuteron d-wave component is obviously taken into account in our calculation. However, these coupled orbital-momentum components of the pair must be summed up coherently.

We assume that such a sum (over the coupled l's) is performed at the present stage, so that the index α', from now on, collectively denotes the set of quantum numbers s, j, t, λ, I, τ, J, J^z, T, and T^z.

Finally, we observe that the direct contribution to the Δ-rescattering term, Eq. (22), vanishes on-shell. (On-shell, the two-nucleon quantum numbers s, j, and t are fixed by the deuteron state, and the relative motion of the spectator q is fixed by total energy conservation.) This vanishing effect is due to isospin considerations, since the intermediate ΔN pair cannot be directly coupled to a final deuteronlike ($t=0$) pair. It does couple, however, through the permutation operator P

in the exchange contribution, as well as through final-state interactions, where one can well have isovector pairs in the intermediate states.

Once the total absorption amplitude $A^{\text{tot}}(q,\alpha',E)$ has been obtained, the pion-absorption excitation function is given by

$$\sigma = \frac{c_{\text{ps}}}{2} \sum_{\alpha'} |A^{\text{tot}}(q,\alpha',E)|^2,$$

(25)

with phase-space factor

$$c_{\text{ps}} = (2\pi)^4 \frac{q}{P_0^\pi} \frac{E_\pi E_t E_N E_d}{(E^{\text{tot}})^2},$$

(26)

where

$$E_\pi = \sqrt{m_\pi^2 + P_0^{\pi 2}},$$

(27)

$$E_t = \sqrt{M_T^2 + P_0^{\pi 2}},$$

(28)

$$E_N = \sqrt{M^2 + q^2},$$

(29)

$$E_d = \sqrt{M_D^2 + q^2},$$

(30)

$$E^{\text{tot}} = E_N + E_d = E_\pi + E_t.$$

(31)

Here, M_D, M_T, are the deuteron and three-nucleon masses, respectively. The momentum q is the on-shell momentum (in c.m. frame) of the outgoing nucleon.

Similarly, the unpolarized differential cross section for the $\pi^+ t \rightarrow pd$ reaction is given by

$$\frac{d\sigma}{d\Omega}(\theta) = \frac{c_{\mathrm{ps}}}{2} \sum_{K,K^z} \left| \sum_{J,J^z,\lambda} C(\lambda KJ; \lambda^z K^z J^z) Y_\lambda^{\lambda^z}(\Omega) \right.$$

$$\times \sum_I (-)^{\lambda-I+K} \hat{K}\hat{I} \begin{Bmatrix} 1 & \frac{1}{2} & K \\ \lambda & J & I \end{Bmatrix}$$

$$\left. \times A^{\mathrm{tot}}(\lambda,I,J,J^z;T,T^z) \right|^2, \tag{32}$$

where K is the channel spin of the deuteron-nucleon system, i.e., the sum of the spins of the two fragments $\mathbf{K}=\mathbf{j}+\boldsymbol{\sigma}$.

Finally, detailed balance gives the expression for the unpolarized cross section for the inverse (pion production) reaction

$$\left[\frac{d\sigma}{d\Omega}(\theta)\right]^{\mathrm{production}} = \frac{1}{3}\left(\frac{P_0^\pi}{q}\right)^2 \left[\frac{d\sigma}{d\Omega}(\theta)\right]^{\mathrm{absorption}}, \tag{33}$$

where θ is the c.m. angle of the deflected particle.

A. Partial-wave absorption amplitudes

We outline here the basic ingredients we used for the calculation of the absorption amplitudes in partial waves. The section is mainly technical and can be ignored on a first reading, if one is not interested in the details of the calculation.

For brevity, out of the four mechanisms discussed previously, we have selected only two mechanisms, namely, the exchange Δ rescattering, which is the dominant one, and the direct IA term. The remaining mechanisms, direct Δ rescattering and exchange IA have a similar structure and do not introduce any novelty.

To avoid unnecessary complications in the formulas, we give here the amplitudes on shell, i.e., we have substituted $|\Phi_d\rangle$ in place of $G_0(E_d)|f_1\rangle$ and have denoted by $u_{lsj}(p) \equiv u(p)$ the s and d component of the deuteron in momentum space. For the inclusion of the three-nucleon dynamics via the AGS equations, these same amplitudes have been extended off shell [see Eq. (18)]. To fix the notation,

the exchange Δ-rescattering amplitude in partial waves can be denoted as

$$B_E^\Delta = 2\sqrt{3}\langle u\alpha'q'|P\hat{\mathcal{A}}_1|\Psi_{\mathrm{BS}},\bar{\alpha},\mathbf{P}_0^\pi\rangle, \tag{34}$$

where q' is the c.m. momentum of the N-d system, $\mathbf{P}_0^\pi$ is the c.m. momentum of the π^+t channel and denotes the beam axis or equivalently the z axis. While the former is a one-dimensional variable in a fully decomposed partial-wave scheme, the latter is three dimensional, since we decompose in partial waves only the baryonic coordinates, not the pionic one. The operator $\hat{\mathcal{A}}_1$ represents the πN-Δ transition on nucleon labeled 2, intermediate Δ propagation, and a ΔN-NN transition between nucleons 2 and 3, while nucleon 1 acts as spectator. The process is diagrammatically illustrated in Fig. 1 of Ref. [17], while P is the three-body permutator previously introduced. For the detailed form of P in partial waves, we used the expression given in the Appendix of Ref. [29].

With α' we collectively denote the quantum numbers for the jI decomposition of the p-d channel listed according to Eq. (3.2) of Ref. [17], while with $\bar{\alpha}$ the quantum numbers for the three-nucleon bound state in the LS scheme are assumed. The details of the calculation in this scheme can be found in Ref. [18], while similar calculations in the jI scheme are found, e.g., in Refs. [30,31].

The resulting expression is

$$\langle u,\alpha',q'|P\hat{\mathcal{A}}_1|\Psi_{\mathrm{BS}},\bar{\alpha},\mathbf{P}_0^\pi\rangle$$

$$= \mathcal{F} \sum_{\substack{kl_1l_1'\alpha''\alpha_\Delta \\ L_\Delta S_\Delta S_z m}} \widetilde{g}(\alpha'\alpha''kl_1l_2l_1'l_2') \mathcal{T}(\alpha''\bar{\alpha})$$

$$\times \mathcal{B}(\alpha''\alpha_\Delta\bar{\alpha}L_\Delta S_\Delta S_z m)$$

$$\times \mathcal{I}_1(\alpha'\alpha''\alpha_\Delta\bar{\alpha}kl_1l_1'L_\Delta S_\Delta S_z m), \tag{35}$$

where

$$\mathcal{F} = \frac{iP_0^\pi(3M+m_\pi)f_{\pi N\Delta}^2 f_{\pi NN}}{72\pi^3 m_\pi^3 (M+m_\pi)\sqrt{\pi\omega_\pi}}, \tag{36}$$

the geometrical coefficients $\widetilde{g}$, $\mathcal{T}$, and $\mathcal{B}$ are given explicitly in the Appendix, and finally

$$\mathcal{I}_1(\alpha'\alpha''\alpha_\Delta\bar{\alpha}kl_1l_1'L_\Delta S_\Delta S_z m) = q'^{l_2+l_2'}\int_0^\infty p'^2 dp' \, p'^{l_1+l_1'} u_{l's'j'}(p') \int_{-1}^1 dx \frac{P_k(x)}{p^{*l''}q^{*\lambda''}} \int_0^\infty p^2 dp \int_{-1}^1 d\cos\hat{\mathbf{P}}$$

$$\times \frac{\mathcal{Q}_{l''l_\Delta}^T(p^*,p_\Delta)}{E+M-\mathcal{M}_\Delta-p_\Delta^2/2\mu_\Delta-q^{*2}/2\nu_\Delta} \Theta_{l_\Delta m}(\cos\hat{\mathbf{P}}_\Delta)\Theta_{\bar{l}m}(\cos\hat{\mathbf{P}})$$

$$\times \int_{-1}^1 d\cos\hat{\mathbf{Q}}' \Theta_{\lambda''n}(\cos\hat{\mathbf{Q}}')\Theta_{\bar{\lambda}n}(\cos\hat{\mathbf{Q}})\Psi_{\bar{\alpha}}(p,q). \tag{37}$$

In this last equation, all the relevant momenta are defined in terms of the channel momenta q' and P_0^π and of the integration variables through the formulas

$$p^* = \sqrt{\tfrac{1}{4} p'^2 + \tfrac{9}{16} q'^2 + \tfrac{3}{4} p' q' x},$$

$$q^* = \sqrt{p'^2 + \tfrac{1}{4} q'^2 - p' q' x},$$

$$p_\Delta = \sqrt{\left(\frac{3M + m_\pi}{6M + 3m_\pi} P_0^\pi\right)^2 + p^2 + 2 \frac{3M + m_\pi}{6M + 3m_\pi} P_0^\pi p \, \cos\hat{\mathbf{P}}},$$

$$\cos\hat{\mathbf{P}}_\Delta = \frac{[(3M + m_\pi)/(6M + 3m_\pi)] P_0^\pi + p \, \cos\hat{\mathbf{P}}}{p_\Delta},$$

$$q = \sqrt{(\tfrac{1}{3} P_0^\pi)^2 + q^{*2} + \tfrac{2}{3} P_0^\pi q^* \, \cos\hat{\mathbf{Q}}'},$$

$$\cos\hat{\mathbf{Q}} = \frac{(1/3) P_0^\pi + q^* \, \cos\hat{\mathbf{Q}}'}{q}. \tag{38}$$

In Eq. (37) $P_k(x)$ represents the Legendre polynomials, $\Theta_{lm}(\cos\theta)$ denotes the associated Legendre functions (normalized according to Ref. [17]), $\mathcal{Q}_{ll'}^T(p, p')$ represents linear combinations of II-kind Legendre polynomials [see Eq. (43) in Ref. [19]], originated by the $\pi + \rho$ meson-exchange diagrams in the tensor ΔN-NN force, and finally $\Psi_{\bar{\alpha}}(p, q)$ is the triton wave function in momentum space and in the LS scheme. In the same equation, it is also assumed that $n = J_z' - S_z - m$, while the identities $l_1 + l_2 = l'$ and $l_1' + l_2' = \lambda'$ hold in both Eqs. (A1) and (37).

Similarly, the direct IA amplitude in partial waves can be expressed as

$$B_D^{\mathrm{IA}} = \sqrt{3} \langle u \alpha' q' | H_{\pi NN} | \Psi_{\mathrm{BS}}, \bar{\alpha}, \mathbf{P}_0^\pi \rangle, \tag{39}$$

with the πNN vertex acting on nucleon 2 as a one-body operator.

The calculation of this matrix element yields

$$\langle u, \alpha', q' | H_{\pi NN} | \Psi_{\mathrm{BS}}, \bar{\alpha}, \mathbf{P}_0^\pi \rangle$$

$$= \mathcal{F}_2 \sum_{L'S'S_z m} \mathcal{B}_2(\alpha' \bar{\alpha} L' S' S_z m) \mathcal{I}_2(\alpha' \bar{\alpha} L' S' S_z m), \tag{40}$$

where

$$\mathcal{F}_2 = \frac{i P_0^\pi (3M + m_\pi) f_{\pi NN}}{2 \pi m_\pi (M + m_\pi) \sqrt{\pi \omega_\pi}} \tag{41}$$

and

$$\mathcal{I}_2(\alpha' \bar{\alpha} L' S' S_z m)$$

$$= \int_0^\infty p'^2 dp' u_{l's'j'}(p') \int_{-1}^1 d \cos\hat{\mathbf{P}}' \Theta_{l'm}(\cos\hat{\mathbf{P}}')$$

$$\times \Theta_{\bar{l}m}(\cos\hat{\mathbf{P}}) \int_{-1}^1 d \cos\hat{\mathbf{Q}}' \Theta_{\lambda'n}(\cos\hat{\mathbf{Q}}')$$

$$\times \Theta_{\bar{\lambda}n}(\cos\hat{\mathbf{Q}}) \Psi_{\bar{\alpha}}(p, q). \tag{42}$$

As in the previous case, all the relevant momenta have to be expressed in terms of the channel momenta q' and P_0^π and of the integration variables

$$p = \sqrt{p'^2 + \left(\frac{3M + m_\pi}{6M + 3m_\pi} P_0^\pi\right)^2 - 2 \frac{3M + m_\pi}{6M + 3m_\pi} P_0^\pi p' \, \cos\hat{\mathbf{P}}'},$$

$$q = \sqrt{q'^2 + (\tfrac{1}{3} P_0^\pi)^2 + \tfrac{2}{3} P_0^\pi q' \, \cos\hat{\mathbf{Q}}'},$$

$$\cos\hat{\mathbf{P}} = \frac{-[(3M + m_\pi)/(6M + 3m_\pi)] P_0^\pi + p' \cos\hat{\mathbf{P}}'}{p},$$

$$\cos\hat{\mathbf{Q}} = \frac{(1/3) P_0^\pi + q' \, \cos\hat{\mathbf{Q}}'}{q}. \tag{43}$$

The coupling coefficient $\mathcal{B}_2$ is explicitly given in the Appendix.

B. 3N bound-state calculation

For the calculation of the three-body bound-state energy E_T and wave function $|\Psi_{\mathrm{BS}}\rangle$ we start from the Lippmann-Schwinger equation

$$|\Psi_{\mathrm{BS}}\rangle = \lim_{\epsilon \to 0} i\epsilon G(E_T + i\epsilon) |\Psi_{\mathrm{BS}}\rangle. \tag{44}$$

Using the resolvent equation

$$G(z) = G_\beta(z) + G_\beta(z) \bar{V}_\beta G(z) \tag{45}$$

and performing the ϵ limit we end up with

$$|\Psi_{\mathrm{BS}}\rangle = G_\beta(E_T)(V - V_\beta) |\Psi_{\mathrm{BS}}\rangle, \tag{46}$$

where V is the total interaction summed over the pairs, V_β is the nuclear interaction of the pair labeled by β, $\bar{V}_\beta$ denotes $V - V_\beta$, and G_β is the channel resolvent for the two-cluster partition.

TABLE I. Ranks of the two-body partial waves of the Paris, Bonn A, and Bonn B potentials in the EST representation.

Partial wave	PEST	BAEST	BBEST
$^1S_0$	5	5	5
$^3S_1 - {}^3D_1$	6	6	6
$^1D_2$	5	4	4
$^3D_2$	5	4	4
$^1P_1$	5	4	4
$^3P_1$	5	4	4
$^3P_0$	5	4	4
$^3P_2 - {}^3F_2$	7	5	5

If we now introduce the position $|F_\beta\rangle = (V - V_\beta) \, |\Psi_{BS}\rangle$ and the relation $V_\gamma G_\gamma = T_\gamma G_0$, we obtain the celebrated equation

$$|F_\beta\rangle = \sum_\gamma \, (1 - \delta_{\beta\gamma}) T_\gamma G_0 |F_\gamma\rangle. \tag{47}$$

Here, the summation runs over all two-fragment partitions γ. The ''form factors'' $|F_\beta\rangle$ are related to $|\Psi_{BS}\rangle$ by

$$|\Psi_{BS}\rangle = \sum_\gamma \, G_0 T_\gamma G_0 |F_\gamma\rangle = \sum_\gamma \, |\Psi_\gamma\rangle, \tag{48}$$

where the $|\Psi_\gamma\rangle$ are the standard Faddeev components. This can be shown by using the definition of $|F_\beta\rangle$ and again the relation $V_\gamma G_\gamma = T_\gamma G_0$:

$$\begin{aligned} |\Psi_\gamma\rangle &= G_0 T_\gamma G_0 |F_\gamma\rangle = G_0 V_\gamma G_\gamma |F_\gamma\rangle \\ &= G_0 V_\gamma G_\gamma (V - V_\gamma) |\Psi_{BS}\rangle = G_0 V_\gamma |\Psi_{BS}\rangle. \end{aligned} \tag{49}$$

The bound-state equation (47) has to be projected onto the three-body partial waves $|pqlbJT\rangle$. In this subsection we use the so-called channel-spin coupling. The label b denotes the set of quantum numbers $(\eta K\lambda)$, where K and λ are the channel spin of the three nucleons [with the coupling sequence $(j,\sigma)K$] and the relative angular momentum between the two-body subsystem and the third particle, respectively. In this paper, the channel-spin coupling K has been already introduced in Eq. (32). Here, the total angular momentum of the three-nucleon system J is given by the coupling sequence (K,λ) while T has been already defined as the total isospin. l is the usual orbital angular momentum and $\eta = (s,j;t)$ collectively denotes the spin, angular momentum [with the coupling sequence $(l,s)j$], and isospin of the two-body subsystem. Defining

TABLE II. Calculated binding energies for the triton. The total angular momentum of the two-body subsystem was restricted to $j \leq 2$. This led to 18 three-body channels in the channel-spin coupling.

BAEST	BBEST	PEST
-8.284	-8.088	-7.3688

$$F_\beta^b(q) = \sum_l \int_0^\infty dp\, p^2 f_l(p) \langle pqlbJT | G_0(E_T) | F_\beta\rangle, \tag{50}$$

inserting the finite-rank form for the T matrix, and using the Pauli principle, we obtain the one-dimensional equation

$$\begin{aligned} F^b(q) = \sum_{b'} \int_0^\infty dq' q'^2 \, \mathcal{A}\mathcal{V}^{bb'}(q,q',E_T) \\ \times \Delta^{\eta'}(E_T - \tfrac{3}{4} q'^2) F^{b'}(q'), \end{aligned} \tag{51}$$

with

$$\begin{aligned} \mathcal{A}\mathcal{V}^{bb'}(q,q',E_T) = 2\sum_{ll'} \int_0^\infty \int_0^\infty dp\, p^2 dp'\, p'^2 f_l(p) \\ \times \langle pqlbJT | G_0(E_T) | p'q'l'b'JT\rangle \\ \times f_{l'}(p'). \end{aligned} \tag{52}$$

The recoupling coefficients for the coupling scheme herein employed can be directly found in Ref. [38], or alternatively, they can be obtained starting from other coupling schemes [29] by means of the usual transformation algebra.

Equation (51) can be treated as an eigenvalue problem. The energy is varied until the corresponding eigenvalue is 1. The ranks for the partial waves taken into account for the bound-state calculations for the different potentials are listed in Table I. Results for the binding energies can be found in Table II.

The whole wave function can now be calculated by either using Eq. (48) or by applying the permutation operator P defined in Eq. (9) on one Faddeev component [29]

$$|\Psi_{BS}\rangle = (1 + P)|\Psi_1\rangle. \tag{53}$$

This second representation has the advantage to be explicitly independent from the T-matrix representation, and is therefore computationally more convenient when the rank of the representation becomes large. The high accuracy of the wave function has been shown in Refs. [33,34].

For the calculation of the Born terms as illustrated in the previous section, the wave function was transformed into the LS scheme via

$$\begin{aligned} \langle [(l\lambda)L,(s\sigma)S]JJ^z | \\ = \sum_{jK} (-1)^{l+s+\lambda+\sigma+L+S+2K} \hat{j}\hat{L}\hat{S}\hat{K} \begin{Bmatrix} l & S & K \\ \sigma & j & s \end{Bmatrix} \\ \times \begin{Bmatrix} l & S & K \\ J & \lambda & L \end{Bmatrix} \langle \{[(ls)j\sigma]K\lambda\}JJ^z |. \end{aligned} \tag{54}$$

C. 3N continuum calculation

In this section we briefly summarize the continuum calculation. As already mentioned the method used here is similar to the techniques developed to incorporate final-state in-

teractions (FSI) in the photodisintegration of triton [23–25,27,28]. The only difference is the inhomogeneity, i.e., the Bornterm, of Eq. (19). Thus, with this replacement our working program for photodisintegration has been easily modified for pion absorption. Both programs are based on a program for n-d scattering [38], which has been rewritten for the EST method used here and the above replacement. The Faddeev results for the continuum presented here are all calculated using a rank-one representation of the two-body t matrices in the kernel of the integral equation. In the case of photodisintegration it has been shown [39] that this is enough for the observables calculated.

In the case of the pion absorption the Born term is much more complicated and has more structure than in the case of photodisintegration. To achieve the required accuracy we used 70 grid points in the q variable for each channel for the off-shell extension of the Born term. For details of the numerical solution of the integral equation we refer to Ref. [40].

III. RESULTS

Our analysis of the $pd \rightarrow \pi^+ t$ reaction is essentially a *parameter-free* analysis, because all the parameters of the model were fixed in previous studies [19,41] on the simpler $\pi^+ d \rightarrow pp$ reaction. This was possible because the character of the calculation is sufficiently microscopic that the tuning parameters are basic quantities such as coupling constants and cutoffs at the meson-baryon vertices. Obviously these very same parameters enter in both $pp \leftrightarrow \pi^+ d$ and $pd \leftrightarrow \pi^+ t$ reactions. We refer to the analyses of Refs. [19,41] for a more detailed discussion on the $\pi^+ d \rightarrow pp$ reaction; here we limit ourselves to summarize few aspects which are specific of this approach. The coupling constants for the Δ-rescattering mechanism are the ones referring to the πNN, $\pi N\Delta$, ρNN, and $\rho N\Delta$ vertices, which were taken from Table B.1 of Ref. [42] (model III). The cutoff parameters (in MeV) of the four vertices are 1600, 900, 1200, and 1350, respectively, which are practically equivalent to the ones given in the same Table B.1 cited above.

In the analysis of pion absorption on deuterons which we used as input for our study, there were only two authentically phenomenological ingredients. First, the way the Δ resonance propagates in the intermediate states, and, second, the off-shell nature of the πNN and $\pi N\Delta$ vertices when the pion is the asymptotic particle, and hence rigorously standing on its mass shell.

Concerning the first point, the resonance peak in the experimental pion-deuteron absorption cross section is below the position of a free Δ (as observed by πN scattering) by a few tenths of MeV. This effect could not be explained within the dynamical model, and therefore the Δ resonance peak has been positioned downwards by introducing an energy shift parameter. Phenomenologically, the magnitude of this shift is of the order of 30–35 MeV; it has, however, to be increased by about 20 MeV (see Refs. [19,41]) if the motion of the other nucleon is taken into account. As for the isobar width, this was fixed to 115 MeV at the resonance, and therefore corresponds to the value of the free resonance width. Note, however, that the resonance peak for pion absorption on deuteron is broader, being around $\Gamma_0 = 150$ MeV [43,44].
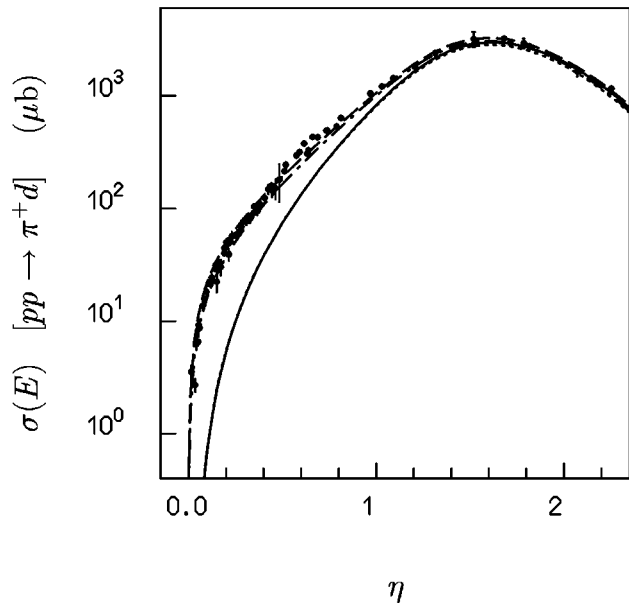

FIG. 1. Excitation function for $\pi^+ d$ production (in μb) from pp collisions. The parameter η corresponds to the pion momentum (c.m.) divided by the pion mass. The full line is the result obtained with Bonn B potential and with p-wave pion-nucleon interactions which includes both isobar and nonisobar degrees of freedom. Practically indistinguishable from the full line, there is a dotted line which correspond to a similar calculation but with Paris potential. The other two curves (dashed and dashed-dotted, respectively) correspond to the inclusion of pion-nucleon final-state interaction in s wave and differ between each other for the NN potential being used. The Bonn B in the dashed case, Paris in the dotted-dashed case.

This broadening of the width is fully described by the $\pi d \rightarrow pp$ model calculation, once all the mechanisms, including FSI, are taken into account.

The second point with a certain deal of phenomenology concerns the off-shell nature of the pion-baryon vertices, in the case where the pion is the asymptotic particle. When the pion is on its mass shell, the extended structure of the πNN and $\pi N\Delta$ vertices may be governed by the nucleon momentum, if the nucleon is the off-shell particle. The importance of including these baryonic off-shell effects has been pointed out also in a recent study of πN scattering [45]. Thus, the two vertices have been endowed with a form factor depending upon the momentum **k** of the interacting nucleon,

$$F_{N,\Delta}(k) = \frac{\lambda_{N,\Delta}^2}{\lambda_{N,\Delta}^2 + k^2}. \qquad (55)$$

For the two-nucleon system k^2 corresponds to the square of the Jacobi coordinate **p**, while for the three-nucleon system, an averaging over angles yields $k^2 \simeq p^2 + 0.25 q^2$.

At the level of the two-nucleon system, the model has been tested against the enormous variety of experimental data collected for the $\pi^+ d \leftrightarrow pp$ reaction, and its strength and weakness, especially at the level of spin observables, have been thoroughly discussed in Refs. [19,41].

To exhibit the quality of the results at the level of the two-nucleon system, we report in Fig. 1 the total production cross section for the $pp \rightarrow \pi^+ d$ reaction from threshold to

TABLE III. Example of three-nucleon partial waves included in our calculation. The notation is $^{2s+1}l_j \; \lambda_I$, where s, l, and j are spin, orbital, and total momentum of the pair, while λ and I are orbital and total momentum for the spectator nucleon. This set of 82 states corresponds to the inclusion of 4 two-nucleon states. In our actual calculation 464 three-body partial waves have been considered, corresponding to the inclusion of 18 two-nucleon states.

$J^P=\frac{1}{2}^-$	$J^P=\frac{1}{2}^+$	$J^P=\frac{3}{2}^-$	$J^P=\frac{3}{2}^+$	$J^P=\frac{5}{2}^-$	$J^P=\frac{5}{2}^+$	$J^P=\frac{7}{2}^-$	$J^P=\frac{7}{2}^+$
$^1S_0P_{\frac{1}{2}}$	$^1S_0S_{\frac{1}{2}}$	$^3S_1P_{\frac{1}{2}}$	$^3S_1S_{\frac{1}{2}}$	$^1D_2P_{\frac{1}{2}}$	$^1D_2S_{\frac{1}{2}}$	$^1D_2P_{\frac{3}{2}}$	$^1D_2D_{\frac{3}{2}}$
$^3S_1P_{\frac{1}{2}}$	$^3S_1S_{\frac{1}{2}}$	$^3D_1P_{\frac{1}{2}}$	$^3D_1S_{\frac{1}{2}}$	$^3S_1P_{\frac{3}{2}}$	$^3S_1D_{\frac{3}{2}}$	$^3S_1F_{\frac{5}{2}}$	$^3S_1D_{\frac{5}{2}}$
$^3D_1P_{\frac{1}{2}}$	$^3D_1S_{\frac{1}{2}}$	$^1D_2P_{\frac{1}{2}}$	$^1D_2S_{\frac{1}{2}}$	$^3D_1P_{\frac{3}{2}}$	$^3D_1D_{\frac{3}{2}}$	$^3D_1F_{\frac{5}{2}}$	$^3D_1D_{\frac{5}{2}}$
$^3S_1P_{\frac{3}{2}}$	$^3S_1D_{\frac{3}{2}}$	$^1S_0P_{\frac{3}{2}}$	$^1S_0D_{\frac{3}{2}}$	$^1D_2F_{\frac{3}{2}}$	$^1D_2D_{\frac{3}{2}}$	$^1D_2F_{\frac{5}{2}}$	$^1D_2D_{\frac{5}{2}}$
$^3D_1P_{\frac{3}{2}}$	$^3D_1D_{\frac{3}{2}}$	$^3S_1P_{\frac{3}{2}}$	$^3S_1D_{\frac{3}{2}}$	$^1S_0F_{\frac{5}{2}}$	$^1S_0D_{\frac{5}{2}}$	$^1S_0F_{\frac{7}{2}}$	$^1S_0G_{\frac{7}{2}}$
$^1D_2P_{\frac{3}{2}}$	$^1D_2D_{\frac{3}{2}}$	$^3D_1P_{\frac{3}{2}}$	$^3D_1D_{\frac{3}{2}}$	$^3S_1F_{\frac{5}{2}}$	$^3S_1D_{\frac{5}{2}}$	$^3S_1F_{\frac{7}{2}}$	$^3S_1G_{\frac{7}{2}}$
$^1D_2F_{\frac{5}{2}}$	$^1D_2D_{\frac{5}{2}}$	$^1D_2P_{\frac{3}{2}}$	$^1D_2D_{\frac{3}{2}}$	$^3D_1F_{\frac{5}{2}}$	$^3D_1D_{\frac{5}{2}}$	$^3D_1F_{\frac{7}{2}}$	$^3D_1G_{\frac{7}{2}}$
		$^3S_1F_{\frac{5}{2}}$	$^3S_1D_{\frac{5}{2}}$	$^1D_2F_{\frac{5}{2}}$	$^1D_2D_{\frac{5}{2}}$	$^1D_2F_{\frac{7}{2}}$	$^1D_2G_{\frac{7}{2}}$
		$^3D_1F_{\frac{5}{2}}$	$^3D_1D_{\frac{5}{2}}$	$^3S_1F_{\frac{7}{2}}$	$^3S_1G_{\frac{7}{2}}$	$^3S_1H_{\frac{9}{2}}$	$^3S_1G_{\frac{9}{2}}$
		$^1D_2F_{\frac{5}{2}}$	$^1D_2D_{\frac{5}{2}}$	$^3D_1F_{\frac{7}{2}}$	$^3D_1G_{\frac{7}{2}}$	$^3D_1H_{\frac{9}{2}}$	$^3D_1G_{\frac{9}{2}}$
		$^1D_2F_{\frac{7}{2}}$	$^1D_2G_{\frac{7}{2}}$	$^1D_2F_{\frac{7}{2}}$	$^1D_2G_{\frac{7}{2}}$	$^1D_2H_{\frac{9}{2}}$	$^1D_2G_{\frac{9}{2}}$
				$^1D_2H_{\frac{9}{2}}$	$^1D_2G_{\frac{9}{2}}$		

above the Δ resonance. The parameter η corresponds to the pion momentum (c.m.), in units of pion mass. The experimental data were extracted from a collection of Refs. [46–55]. All data have been converted into production data using the principle of detailed balance, if necessary, and in case of the data of Ref. [46], charge-independence considerations were applied. The full line is the result obtained with the Bonn B potential, and with the p-wave pion-nucleon mechanisms which, as discussed in the previous section, include both isobar and nonisobar degrees of freedom. Practically indistinguishable from the full line there is a dotted line corresponding to a similar calculation but with the Paris potential. The differences between the two curves slightly increase with energy and at the resonance peak the Paris result is less than 5% smaller than the Bonn B one.

The other two curves (dashed and dashed dotted, respectively) correspond to the additional inclusion of s-wave pion-nucleon interactions in the final state of the production process (or conversely in the initial state, for pion absorption). The leading contribution for this πN-πN interaction was obtained via a ρ-meson exchange model in Ref. [41]. The two curves differ in the choice of the NN potential, the Bonn B being referred to by the dashed line, the Paris by the dotted-dashed curve.

The log scale emphasizes the threshold results, and shows that in order to achieve a correct reproduction of data over three orders of magnitude, the pion-nucleon interactions via ρ-meson exchange have to be considered as well. Note, however, that the process around the Δ resonance is dominated by the p-wave mechanisms which are triggered by the πNN and $\pi N\Delta$ vertices. On a linear scale, the threshold effects in pion production due to the s-wave mechanisms would appear smaller.

At this stage of our study of the $pd\leftrightarrow\pi^+t$ process, we have excluded the ρ-mediated pion-nucleon interaction in s wave, and limited the analysis around the Δ resonance. Further work is needed to include the low-energy mechanisms, and to extend the calculation at the production threshold. In what follows we considered pion-nucleon interactions in p

waves only. However, both Δ and non-Δ degrees of freedom were considered. We note, however, that we treat the pion-nucleus wave three dimensionally and carefully calculate the relevant kinematical transformations from the pion-nucleus to the pion-nucleon variables. This requires additional integrations over angular variables in order to produce the absorption amplitudes [see Eqs. (37) and (42)]. And, because of this, the total angular momentum J is not restricted, neither is the parity P, and thus we have taken into account a few J^P states: $J=(\frac{1}{2})^\pm$, $J=(\frac{3}{2})^\pm$, $J=(\frac{5}{2})^\pm$, and $J=(\frac{7}{2})^\pm$. For each of these three-body quantum numbers, one should consider in principle an infinite set of partial waves for the two-body subsystem, which matches a corresponding infinite set of partial waves for the spectator particle to give a fixed J^P. Clearly, a truncation over a limited number of states is nec-
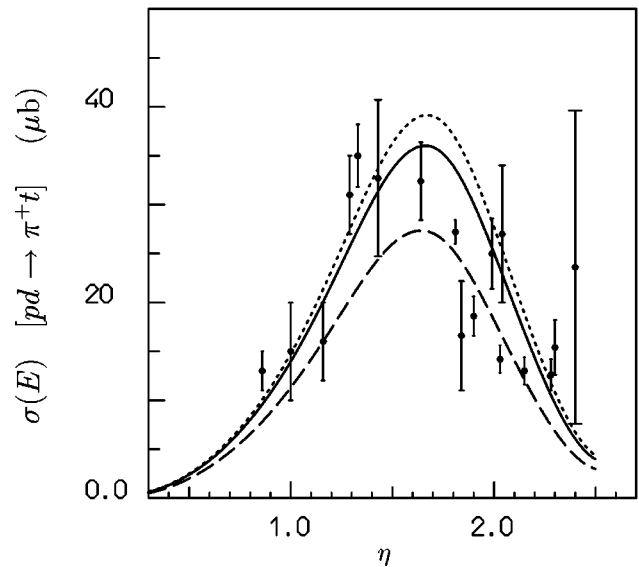

FIG. 2. Excitation function of pion production via proton-deuterium collisions (in μb). The calculation includes also Δ excitation and has been performed with the same parameters as in Fig. 1.
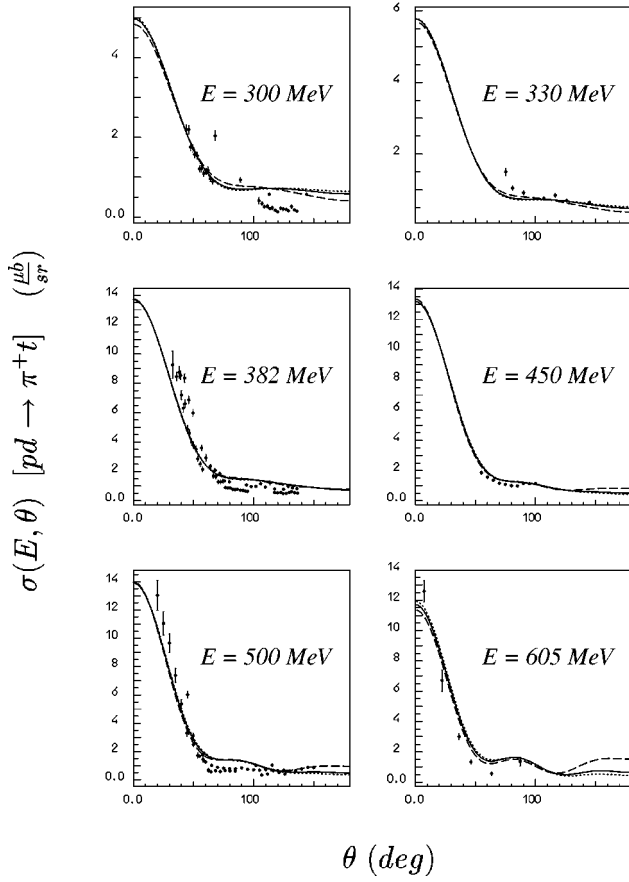
FIG. 3. Differential cross section for π^+ production in the proton-deuterium collision.

essary. Table III shows the smallest set of three-body partial waves which have been included in our calculation. Here, four two-nucleon states have been included, namely, $^1S_0$, $^3S_1$, $^3D_1$, and $^1D_2$, while the maximum values considered for the orbital and angular momentum of the *spectator* were $\lambda = 5$ and $I = \frac{9}{2}$, respectively, for a total amount of 82 states. Such three-body states are indicated in the table according to the notation $^{2s+1}l_j$ λ_I.

All our calculations, unless otherwise explicitly indicated, have been performed with a much larger set. In particular, in calculating the matrix elements of the absorption/production matrix elements with exchange operator, we took into account 18 two-body partial waves $^1S_0$, $^3S_1$, $^3D_1$, $^1D_2$, $^3P_0$, $^1P_1$, $^3P_1$, $^3D_2$, $^3P_2$, $^3F_2$, $^1F_3$, $^3D_3$, $^3G_3$, $^3F_3$, $^3G_4$, $^1G_4$, $^3F_4$, and $^3H_4$. This, with the same cuts in the spectator quantum numbers λ and I specified as before, yields 34 channels for $J^P = (\frac{1}{2}^\pm)$, 58 for $J^P = (\frac{3}{2}^\pm)$, 70 for $J^P = (\frac{5}{2}^\pm)$, and 70 for $J^P = (\frac{7}{2}^\pm)$ for a grand total of 464 three-body states. In solving the Faddeev equations for the three-nucleon dynamics in the p-d channel, of the 18 nucleon-nucleon waves we have included the first 10 states ($j \leq 2$) since for these the NN state-dependent interaction was available.

Figure 2 shows the integral cross section (in μb) of the $pd \rightarrow \pi^+ t$ reaction around the resonance. The x-axis dependence is upon the parameter η, which has been previously defined. The experimental bars were obtained with the help of a collection of data contained in Refs. [56,57]. To this collection, we have added the experimental results of Ref.

TABLE IV. Calculated production cross sections (in μb) at $\eta = 1.36$ for various NN potentials. The impulse approximation (first row) represents a bare plane-wave calculation without Δ rescatterings. The second and third rows include also the Δ degrees of freedom but use a plane-wave approximation in the incoming channel. They differ between each other for the number of partial waves included in the intermediate states. In case a, four two-nucleon states have been included and only S-wave orbital momentum for the intermediate Δ-nucleon state has been considered. In case b, 18 two-nucleon states and intermediate Δ-nucleon states in S, P, and D waves have been taken into account. In the last two rows, where the same number of partial waves have been included as in the previous two, the p-d interactions in the initial state have been included via a Faddeev calculation.

	Bonn A	Bonn B	Paris
IA	0.58	0.72	0.93
PWa	30.1	28.0	21.7
PWb	30.7	28.7	22.5
ISIa	31.3	29.0	22.5
ISIb	32.0	29.9	23.4

[58] for π^- absorption on ^{3}He at 64 and 119 MeV, assuming time reversal and charge symmetry. The full, dotted, and dashed lines differ among each other for the NN potential which has been used to generate the asymptotic bound states, i.e., the deuteron and triton. The three curves represent calculations with Bonn B (solid line), Bonn A (dotted), and Paris interactions. We find that at the peak the Paris results are smaller than the Bonn B results by almost 25%. This relative difference is substantially larger than the 5% difference obtained for the simpler $pp \rightarrow \pi^+ d$ reaction. Experimentally, the $pd \rightarrow \pi^+ t$ cross section is smaller by a factor $80-85$ with respect to the $pp \rightarrow \pi^+ d$ one. This large suppression, due to the small overlap of the deuteron wave function in the incoming channel with the pion production matrix elements, is fully reproduced by our calculations.

The unpolarized differential cross section is reported in Fig. 3 for a variety of energies spanning the Δ resonance. While Fig. 2 shows the normalization of the cross section, in Fig. 3 we have addressed our attention to the pure angular dependence and therefore all the curves are normalized to the experimental data. Thus, the three curves referring to 300 MeV (lab energy of the proton) have been multiplied by a factor. The full line, referring to the result with Bonn B potential, has been multiplied by 1.075, the dotted line (Bonn A) by 1.016, and the dashed line (Paris) by 1.329. The three factors are due to the differences in normalization immediately perceived in Fig. 2 for $\eta = 1$, which is the corresponding value for that energy.

At the resonance peak, the angular differences between the various NN potentials are practically zero. These differences, however, increase in moving away from the resonance in both directions. We find larger differences above the resonance, for backward angles. In particular, calculations with Paris potential seem to reproduce better the data at backward angles.

In the first sector ($E = 300$ MeV) of the figure, the data were taken from the inverse absorption reaction, π^- ^{3}He$\rightarrow nd$ at 64 MeV, Ref. [58], using the detailed balance
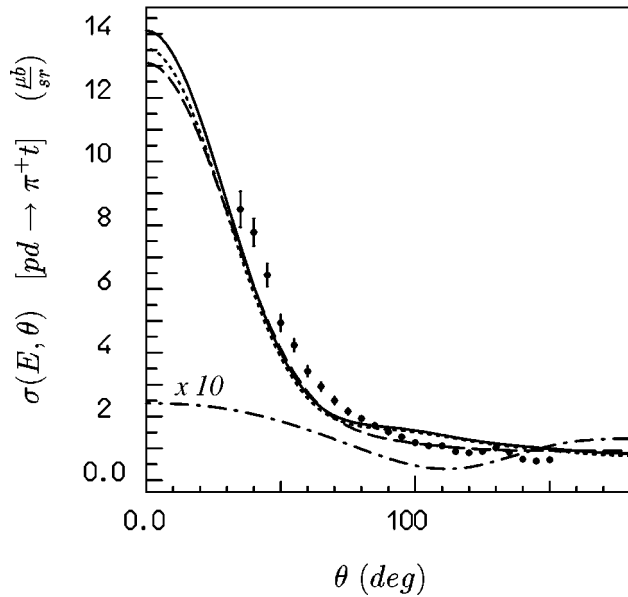
FIG. 4. π^+-production differential cross section at $\eta = 1.36$. The full line shows the results with inclusion of nucleon-nucleon initial-state interactions. The dotted line represents the plane-wave calculation. The dashed line shows the results with a limited number of channels. The dashed-dotted line shows the contribution of the sole nonisobar degrees of freedom, magnified by a factor 10. All calculations were performed with the Paris potential.

and charge symmetry. In the same picture we have reported also four points obtained from Ref. [63] for the production reaction at 305 MeV. The four points are clearly visible because they stand above the rest of the data set. From the same reference [63], we have taken also the data at 330 MeV, shown in the second sector, while the data at 382 MeV were obtained from pion-absorption reactions at 119 MeV. In particular, data from both reactions $\pi^- \, {}^3\text{He} \rightarrow nd$ (Ref. [58]) and $\pi^+ t \rightarrow pd$ (Ref. [59]) have been included. The data at 450 and 500 MeV were taken from Ref. [60] using charge independence, and finally, at 605 MeV, we considered the older data of Ref. [61]. In terms of integrated cross section, that last set of angular data corresponds in Fig. 2 to the datum at $\eta = 2.4$, which has the largest error bar. Because of this, the large multiplicative factors we found at this energy (5.956 for Bonn B, 5.413 for Bonn A, and 7.982 for Paris) seem to be attributable more to normalization problems in the data, than to the model calculation. For all the remaining energies, the normalization factors were all well around one.

Table IV compares for the three NN potentials the integrated cross section calculated under various conditions. The first row exhibits the contribution arising from the sole πNN vertex (denoted IA, impulse approximation). In the second row (PWa), we show a plane-wave calculation which includes the isobar degrees of freedom via the $\pi N\Delta$ vertex. In the third row, PWb, the number of intermediate NN states have been increased from 4 up to 18 two-body partial waves, and from the sole S state up to the D states in the ΔN orbital momentum. The effect in the total cross section is about 3%; however, as shown in the next figure, there is a not large but sizeable change in the angular dependence. In a forthcoming article we will show that certain spin observables such as A_{y0} are extremely sensitive to the number of waves included in the intermediate states.
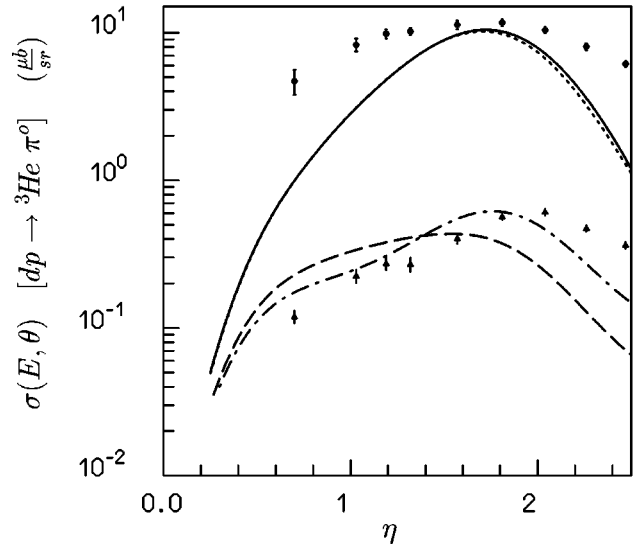
FIG. 5. Unpolarized differential cross section for π^0 production in proton-deuterium collisions. Circles and triangles represent measurements taken at Saturne [62] at forward and backward (c.m.) angles, respectively. The solid and broken curves are forward-angle calculations with Bonn B and Paris potentials, respectively, the dashed and dotted-dashed curves are the corresponding backward-angle results.

Finally, in the last two rows (ISIa and ISIb) the effect of three-nucleon dynamics in the incoming channel has been taken into account with the Faddeev formalism. Similar to the previous two rows, these differ between each other for the number of intermediate states. In both cases, the effect of the three-nucleon dynamics yields an increase of about 4% or less. Around the same value for η, the $pd \rightarrow \pi^+ t$ cross section extracted from Ref. [60] gives 35 ± 3.2 μb at $\eta = 1.32$, while data extraction from [58] gives 32.7 ± 8.0 at $\eta = 1.43$.

Figure 4 shows the differential cross section calculated for $\eta = 1.36$ in various conditions, in comparison to the data obtained for π^0 production at 350 MeV assuming charge independence [60]. The solid line is the solution of the Faddeev equation for the three-nucleon dynamics in the incoming channel. The corresponding plane-wave results are shown by the dotted line. The comparison shows that the three-nucleon dynamics have a relatively small effect on the differential cross section. On a linear scale, the effect is more pronounced at forward angles, however, on a log scale it becomes evident that the overall effect is simply a rescaling of the curve, without changing the angular dependence. The dashed line shows the results obtained with a limited number of channels (a total of 82 instead of 464). Differences are seen at both forward and backward angles. It is therefore important to consider convergence with respect to the number of three-body states included in the calculation. Finally, the dashed-dotted line contains the effect of the sole nucleonic intermediate states. For reasons of visibility, these nonisobaric effects have been multiplied by a factor of 10. Overall the effect is small, but at backward angles its contribution is larger than 10%. The calculations shown in the figure were performed with the Paris interaction. Practically identical angular dependences have been obtained with the Bonn B and Bonn A potentials.

Finally, Fig. 5 exhibits the dependence of the differential cross section upon the parameter η for forward and backward angles. Due to the smallness of the three-body effects, the calculations have been performed in plane-wave approximation. The theoretical results have been divided by 2 for comparison with the experimental data for π^0 production obtained at Saclay [62]. The Bonn B and Paris curves have been normalized at E=350 MeV to the data of Ref. [60].

IV. SUMMARY AND CONCLUSIONS

We analyzed the $pd \to \pi^+ t$ reaction around the Δ resonance with a model calculation which explicitly includes isobar degrees of freedom and meson-exchange diagrams. The elementary production/absorption mechanisms were tested on the simpler $pp \to \pi^+ d$ reaction. In particular, the position and width of the isobar resonance were modeled to reproduce the excitation function of the $pp \to \pi^+ d$ process, and off-shell effects in the baryonic coordinates were taken into account in both πNN and $\pi \Delta N$ vertices. The same absorption mechanisms (without further changes) have been embedded in a Faddeev-based treatment for the $pd \to \pi^+ t$ process, where the three-nucleon bound state and the three-nucleon continuum dynamics in the initial channel were calculated using the Faddeev-AGS formalism. The computational method is similar to the one employed recently for the triton photodisintegration. We checked our results against integral and differential cross-section data in the resonance region, finding that the unpolarized experimental data are reproduced reasonably well.

As for the excitation function, we found that the resonance peak is reproduced within the errors without changing the isobar parameters in passing from pp pion production to the pd one. We also found that the magnitude of the curve (i.e., the normalization of the cross section) is sensitive to the nucleon-nucleon interaction used as input for the $3N$ bound-state wave function, with a 25% difference between the Bonn potentials and the Paris one. This sensitivity is larger by a factor of 5 with respect to the $pp \to \pi^+ d$ process. The results with the Paris potential were always smaller than those obtained with the Bonn potentials.

We then analyzed the angular dependence of the differential cross section in the energy region spread around the resonance peak. At the peak there are practically no differences in the angular distribution with respect to the model selected for the nucleon-nucleon interaction. In moving away from the peak, the angular distributions begin to show some interaction dependence: the differences are larger at higher energies and backward angles. The calculation with the Paris potential seems slightly in better agreement with the general trend of the data at backward angles. Definitive conclusions, however, should be drawn only after the πN interactions in s wave are also included.

At the resonance peak we have singled out the role of the nonisobaric πN interaction in p wave (the IA term), analyzed the convergence of the calculation with respect to the number of intermediate three-baryon partial waves included, and considered the effect of the three-body dynamics in the nucleon-deuteron channel. It turns out that the size of these effects are all comparable. Indeed, the contribution of the IA term with respect to the total cross section ranges from 2 to

4% depending on the model interaction which has been used. Differences of the same size are found when the calculation performed with a strictly necessary set of partial waves is compared with converged results. Finally, by means of the Faddeev-AGS formalism, it was possible to ascribe a 4% effect to the contribution due to the three-nucleon dynamics in the nucleon-deuteron channel. It is obvious that this is equivalent to saying that for the inverse pion-absorption reaction, final state interactions contribute with the same 4% amount.

In conclusion, we have here confirmed the expectations, previously formulated in Refs. [17,64], that a careful embedding of the basic pion absorption/production matrix elements in a Faddeev-based treatment of the few-nucleon dynamics is a very important tool for understanding the hadronic processes in nuclei at intermediate energies. Once this point has been settled, it will be possible to move further on with the same approach and tackle other, more refined experimental data underlining the pion few-nucleon systems.

Such aspects are, e.g., the pionic absorption on the diproton [65], the wealth of experimental data involving polarization phenomena [6,60,63,66], the pion-induced reaction at energies around the pionic threshold [67], and, finally, the meson-absorption coincidence experiments (π^+,pp) at nonconjugated angles with the connected puzzle of the "genuine" three-body mechanisms [68]. However, before all of these aspects can be theoretically disentangled, an important improvement is needed in our treatment (as well as in any other approach). This is connected with the role played by the pion-nucleon s-wave interaction (in both its isoscalar and isovector components) in multiple rescattering processes. Stated in other words, it is the role played by the pion-nucleus final state interaction (or initial, depending on the selected direction in time). This aspect is still missing in the present treatment of the $d(p, \pi^+)$t process, but a flavor of its importance can be immediately percieved in the simpler case of the $p(p, \pi^+)d$ reaction, by glancing at the dashed and dotted-dashed curves passing through the data in Fig. 1.

APPENDIX

We collect here the detailed expressions for the coupling coefficients necessary for the calculation of the partial-wave amplitudes given in Sec. II A.

In the case of the exchange Δ-rescattering diagram, Eq. (35), the coefficients are

$$\widetilde{g}(\alpha\alpha' k l_1 l_2 l_1' l_2') = -\hat{l}\hat{s}\hat{j}\hat{t}\hat{\lambda}\hat{I}\hat{l}'\hat{s}'\hat{j}'\hat{t}'\hat{\lambda}'\hat{I}' \begin{Bmatrix} \frac{1}{2} & \frac{1}{2} & t \\ \frac{1}{2} & T & t' \end{Bmatrix} \sum_{LS} (-)^L \hat{L}^2 \hat{S}^2 \begin{Bmatrix} \frac{1}{2} & \frac{1}{2} & s \\ \frac{1}{2} & S & s' \end{Bmatrix} \begin{Bmatrix} l & s & j \\ \lambda & \frac{1}{2} & I \\ L & S & J \end{Bmatrix} \begin{Bmatrix} l' & s' & j' \\ \lambda' & \frac{1}{2} & I' \\ L & S & J \end{Bmatrix}$$

$$\times (-)^{k+\lambda'+l_1'} \left(\frac{1}{2}\right)^{l_1+l_2'} \left(\frac{3}{4}\right)^{l_2}$$

$$\times \sqrt{\frac{(2l'+1)!}{(2l_1)!(2l_2)!}} \sqrt{\frac{(2\lambda'+1)!}{(2l_1')!(2l_2')!}} \sum_{ff'} \hat{f}\hat{f}' C(l_1 l_1' f; 000) C(lfk; 000) C(l_2 l_2' f'; 000) C(\lambda f' k; 000)$$

$$\times \begin{Bmatrix} l & f & k \\ f' & \lambda & L \end{Bmatrix} \begin{Bmatrix} l_1 & l_2 & l' \\ l_1' & l_2' & \lambda' \\ f & f' & L \end{Bmatrix}, \tag{A1}$$

$$\mathcal{T}(\alpha'\,\overline{\alpha}) = 96\sqrt{30}(-)^{s'+j'+1+\overline{s}+\overline{t}} \hat{s}'\hat{I}'\hat{j}'\hat{t}'\hat{I}'\,\hat{\overline{s}}\,\hat{\overline{S}}\,\hat{\overline{t}}\,\hat{\overline{T}} \begin{Bmatrix} t' & \frac{1}{2} & \frac{1}{2} \\ 1 & \frac{3}{2} & \frac{1}{2} \end{Bmatrix} \begin{Bmatrix} \frac{1}{2} & \overline{t} & t' \\ \frac{1}{2} & T' & \overline{T} \end{Bmatrix} \begin{Bmatrix} 1 & \frac{1}{2} & \frac{3}{2} \\ \frac{1}{2} & t' & \overline{t} \end{Bmatrix} C(1\overline{T}T'; 1-\frac{1}{2}\,\frac{1}{2}), \tag{A2}$$

$$\mathcal{B}(\alpha'\,\alpha_\Delta\,\overline{\alpha}L_\Delta S_\Delta S_z m) = (-)^{s_\Delta+S_\Delta+\overline{T}} i^{l_\Delta-l'} \hat{s}_\Delta^2 \hat{l}_\Delta \hat{S}_\Delta \hat{L}_\Delta \begin{pmatrix} l' & 2 & l_\Delta \\ 0 & 0 & 0 \end{pmatrix} \begin{Bmatrix} 1 & \frac{1}{2} & \frac{3}{2} \\ \frac{1}{2} & s_\Delta & \overline{s} \end{Bmatrix} \begin{Bmatrix} 1 & \overline{s} & s_\Delta \\ \frac{1}{2} & S_\Delta & \overline{S} \end{Bmatrix} \begin{Bmatrix} j' & s' & l' \\ 2 & l_\Delta & s_\Delta \end{Bmatrix}$$

$$\times \begin{Bmatrix} \frac{1}{2} & \frac{3}{2} & 1 \\ \frac{1}{2} & \frac{1}{2} & 1 \\ s' & s_\Delta & 2 \end{Bmatrix} \begin{Bmatrix} l_\Delta & s_\Delta & j' \\ \lambda' & \frac{1}{2} & I' \\ L_\Delta & S_\Delta & J' \end{Bmatrix} C(L_\Delta S_\Delta J'; (J_z'-S_z)S_z J_z') C(\overline{L}\,\overline{S}\,\overline{J}; (J_z'-S_z)S_z J_z')$$

$$\times C(1\,\overline{S}S_\Delta; 0 S_z S_z) C(l_\Delta \lambda' L_\Delta; m(J_{z'}-S_z-m)(J_z'-S_z)) C(\overline{l}\,\overline{\lambda}\,\overline{L}; m(J_z'-S_z-m)(J_z'-S_z)). \tag{A3}$$

Similarly, the recoupling coefficient for the direct IA mechanism, Eq. (40), is

$$\mathcal{B}_2(\alpha'\,\overline{\alpha}L'S'S_z m) = (-)^{1+\overline{s}+s'+\overline{t}+t'+S'+T'} \hat{\overline{s}}\,\hat{s}'\,\hat{\overline{t}}\,\hat{t}'\hat{\overline{S}}\,\hat{\overline{T}}\,\hat{j}'\,\hat{I}'\,\hat{L}'$$

$$\times \hat{S}' \begin{Bmatrix} \frac{1}{2} & \overline{t} & t' \\ \frac{1}{2} & T' & \overline{T} \end{Bmatrix} \begin{Bmatrix} 1 & \frac{1}{2} & \frac{1}{2} \\ \frac{1}{2} & t' & \overline{t} \end{Bmatrix} C\left(1\overline{T}T'; 1-\frac{1}{2}\,\frac{1}{2}\right) \begin{Bmatrix} \frac{1}{2} & \overline{s} & s' \\ \frac{1}{2} & S' & \overline{S} \end{Bmatrix} \begin{Bmatrix} 1 & \frac{1}{2} & \frac{1}{2} \\ \frac{1}{2} & s' & \overline{s} \end{Bmatrix}$$

$$\times \begin{Bmatrix} l' & s' & j' \\ \lambda' & \frac{1}{2} & I' \\ L' & S' & J' \end{Bmatrix} C(L'S'J'; (J_z'-S_z)S_z J_z') C(\overline{L}\,\overline{S}\,\overline{J}; (J_z'-S_z)S_z J_z') C(1\,\overline{S}S'; 0 S_z S_z)$$

$$\times C(l'\lambda' L'; m(J_z'-S_z-m)(J_z'-S_z)) C(\overline{l}\,\overline{\lambda}\,\overline{L}; m(J_z'-S_z-m)(J_z'-S_z)). \tag{A4}$$

In all equations, we have assumed $\hat{j} = \sqrt{2j+1}$.

---

[1] J. M. Eisenberg and D. S. Koltun, *Theory of Meson Interactions with Nuclei* (Wiley, New York, 1980), p. 305.

[2] M. Ruderman, Phys. Rev. **87**, 383 (1952).

[3] C. H. Q. Ingram, N. W. Tanner, J. J. Domingo, and J. Rohlin, Nucl. Phys. **B31**, 331 (1971).

[4] H. W. Fearing, Phys. Rev. C **11**, 1210 (1975); **11**, 1493 (1975); **16**, 313 (1977).

[5] M. P. Locher and H. J. Weber, Nucl. Phys. **B76**, 400 (1974).

[6] W. R. Falk, Phys. Rev. C **50**, 1574 (1994).

[7] D.V. Bugg, A. Hasan, and R. L. Shypit, Nucl. Phys. **A477**, 546 (1988); D. V. Bugg, *ibid.* **A437**, 534 (1985).

[8] A. M. Green and E. Maqueda, Nucl. Phys. **A316**, 215 (1979).

[9] A. M. Green and M. E. Sainio, Nucl. Phys. **A329**, 477 (1979).

[10] M. E. Sainio, Nucl. Phys. **A389**, 477 (1979).

[11] J. M. Laget and J. F. Lecolley, Phys. Lett. B **194**, 177 (1987).

[12] G. Backenstoss *et al.*, Phys. Rev. Lett. **55**, 2782 (1985).

[13] T. Alteholz *et al.*, Phys. Rev. Lett. **73**, 1336 (1994).

[14] G. Backenstoss *et al.*, Phys. Lett. B **379**, 60 (1996).

[15] G. Audit *et al.*, Nucl. Phys. **A614**, 461 (1997).

[16] L. Canton, G. Cattapan, P. J. Dortmans, G. Pisent, W. Schadow, and J. P. Svenne, in *Proceedings of the VI Workshop on Theoretical Nuclear Physics Problems*, edited by I. Bombaci, A. Bonaccorso, A. Fabrocini, A. Kviesky, S. Rosati, and M. Viviani, Cortona, Italy, 1995 (unpublished), p. 45.

[17] L. Canton, J. P. Svenne, and G. Cattapan, Phys. Rev. C **48**, 1562 (1993).

[18] Ch. Hajduk, P. U. Sauer, and W. Strueve, Nucl. Phys. **A405**, 581 (1983).

[19] L. Canton, G. Cattapan, P. J. Dortmans, G. Pisent, and J. P. Svenne, Can. J. Phys. **74**, 209 (1996).

[20] B. G. Ritchie, Phys. Rev. C **28**, 926 (1983).

[21] H. Sugawara and F. von Hippel, Phys. Rev. **172**, 1764 (1968).

[22] M. Gari, G. Niephaus, and B. Sommer, Phys. Rev. C **23**, 504 (1981).

[23] W. Sandhas, Few-Body Syst. Suppl. **1**, 64 (1986).

[24] W. Schadow, J. Richter, and W. Sandhas, in *14th International IUPAP Conference on Few Body Problems in Physics*, edited by F. Gross (CEBAF, Virginia, 1994), p. 695.

[25] W. Schadow and W. Sandhas, Phys. Rev. C **55**, 1074 (1997).

[26] E. O. Alt, P. Grassberger, and W. Sandhas, Nucl. Phys. **B2**, 167 (1967).

[27] I. M. Barbour and A. C. Phillips, Phys. Rev. C **1** 175 1970.

[28] B. F. Gibson and D. H. Lehman, Phys. Rev. C **11**, 29 (1975).

[29] D. Hüber, H. Kamada, H. Witała, and W. Glöckle, Few-Body Syst. **16**, 165 (1994).

[30] T. Sasakawa and S. Ishikawa, Few-Body Syst. **1**, 3 (1986).

[31] W. Glöckle *The Quantum Mechanical Few-Body Problem* (Springer, Berlin, 1993).

[32] D. J. Ernst, C. M. Shakin, and R. M. Thaler, Phys. Rev. C **8**, 46 (1973); **9**, 1780 (1974).

[33] W. C. Parke, Y. Koike, D. R. Lehman, and L. C. Maximon, Few-Body Syst. **11**, 89 (1991).

[34] W. Schadow, W. Sandhas, and J. Haidenbauer (unpublished).

[35] J. Haidenbauer and Y. Koike, Phys. Rev. C **34**, 1187 (1986).

[36] Y. Koike, J. Haidenbauer, and W. Plessas, Phys. Rev. C **41**, 396 (1987).

[37] T. Cornelius, W. Glöckle, J. Haidenbauer, Y. Koike, W. Plessas, and H. Witała, Phys. Rev. C **41**, 2538 (1990).

[38] Th. Januschke, T. Frank, W. Sandhas, and H. Haberzettl, Phys. Rev. C **47**, 1401 (1993).

[39] W. Schadow and W. Sandhas (unpublished).

[40] Th. Januschke, Ph.D. thesis, Universität Bonn, 1990.

[41] P. J. Dortmans, L. Canton, and K. A. Amos, J. Phys. G **23**, 479 (1997).

[42] R. Machleidt, Adv. Nucl. Phys. **19**, 189 (1989).

[43] T. Ericson and W. Weise, *Pions and Nuclei* (Claredon, Oxford, 1988).

[44] B. G. Ritchie, Phys. Rev. C **28**, 926 (1983).

[45] C. Schütz, J. W. Durso, K. Holinde, and J. Specht, Phys. Rev. C **49**, 2671 (1994).

[46] D. A. Hutcheon *et al.*, Nucl. Phys. **A535**, 618 (1991).

[47] P. Heimberg *et al.*, Phys. Rev. Lett. **77**, 1012 (1996).

[48] Carl M. Rose, Jr., Phys. Rev. **77**, 1305 (1967).

[49] B. G. Ritchie, T. D. Averett, D. Rothenberger, J. R. Tinsley, R. C. Minehart, K. Giovanetti, L. C. Smith, G. S. Blanpied, and B. M. Preedom, Phys. Rev. C **47**, 21 (1993).

[50] B. G. Ritchie *et al.*, Phys. Rev. C **24**, 552 (1981).

[51] B. G. Ritchie *et al.*, Phys. Rev. C **27**, 1685 (1983).

[52] S. I. Gogolev *et al.*, Phys. Lett. B **300**, 24 (1993).

[53] D. Axen, G. Duesdieker, L. Felawka, Q. Ingram, and R. Johnson, Nucl. Phys. **A256**, 387 (1976).

[54] C. Richard-Serre, W. Hirt, D. F. Meadsday, E. G. Michaelis, M. J. M. Saltmarch, and P. Skarek, Nucl. Phys. **B20**, 413 (1970).

[55] J. Boswell, R. Altemus, R. Minehart, L. Orphanos, H. J. Ziock, and E. A. Wadlinger, Phys. Rev. C **25**, 2540 (1982).

[56] H. Machner, Acta Phys. Pol. B **24**, 1555 (1993).

[57] H. Machner, in *Proceedings of the 5th International Symposium on Meson-Nucleon Physics and the Structure of the Nucleon*, edited by G. Höler, W. Kluge, and B. M. K. Nefkens, Boulder, Colorado, 1993 (unpublished), Vol. I, p. 127.

[58] P. Weber *et al.*, Nucl. Phys. **A534**, 541 (1991); (private communications).

[59] P. Salvisberg *et al.*, Phys. Rev. C **46**, 2172 (1992).

[60] J. M. Cameron, P. Kitching, J. Pasos, J. Thekkumthala, R. Abegg, D. A. Hutcheon, C. A. Miller, S. A. Elbakr, and A. H. Hussein, Nucl. Phys. **A472**, 718 (1987).

[61] E. Aslanides *et al.*, Phys. Rev. Lett. **39**, 1654 (1977).

[62] C. Kerboul *et al.*, Phys. Lett. B **181**, 28 (1986); B. Mayer (private communication).

[63] G. J. Lolos, E. L. Mathie, G. Jones, E. G. Auld, G. Giles, B. McParland, P. L. Walden, W. Ziegler, and W. R. Falk, Nucl. Phys. **A386**, 477 (1982).

[64] G. Cattapan and L. Canton, Phys. Rev. C **44**, 1784 (1991).

[65] H. Toki and H. Sarafian, Phys. Lett. **119B**, 285 (1982); K. Otha, M. Thies, and T.-S. H. Lee, Ann. Phys. (N.Y.) **163**, 420 (1985); R. R. Silbar and E. Piasetzky, Phys. Rev. C **29**, 1116 (1984); O. V. Maxwell and C. Y. Cheung, Nucl. Phys. **A454**, 606 (1985); D. Zucić and N. Šimičević, Few-Body Syst. **8**, 95 (1990); J. A. Niskanen, Phys. Rev. C **43**, 36 (1991).

[66] J. A. Niskanen, in Proceedings of the Fifth International Symposium on Polarization Phenomena in Nuclear Physics, Santa Fe, 1980, AIP Conf. Proc. No. 69 (AIP, New York, 1981), p. 62; E. G. Auld, in Proceedings of the Fifth International Symposium on Polarization Phenomena in Nuclear Physics, Santa Fe, 1980, AIP Conf. Proc. No. 69 (AIP, New York, 1981), p. 93.

[67] A. Boudard *et al.*, Phys. Lett. B **214**, 6 (1988); M. A. Pickar, A. D. Bacher, H. O. Meyer, R. E. Pollock, and G. T. Emery, Phys. Rev. C **46**, 397 (1992); V. N. Nikulin *et al.*, *ibid.* **54**, 1732 (1996).

[68] H. J. Weyer, Phys. Rep. **195**, 295 (1990); C. H. Q. Ingram, Nucl. Phys. **A553**, 573c (1993).